Removal of Cr^{3+} ions from a model solution by HCl treated *Artocarpus heterophyllus* L. seeds: Equilibrium and Kinetic study

Nthiga, Esther Wanja[1], Ndung'u, Samuel Ng'ang'a[2], Kibet, Kelvin[1], Wanjau, Ruth Nduta[2]
[1]*Department of Chemistry, Dedan Kimathi University of Technology, P.O Box 657-10100, Nyeri, Kenya*
[2]*Department of Chemistry, Kenyatta University, P.O Box 43844-0100, Nairobi, Kenya*

Abstract:- **The present study used Jackfruit seeds (JS) as a novel adsorbent in adsorption of Cr^{3+} ions from an aqueous solution. A modified Jackfruit seeds (MJS) adsorbent was prepared by chemical treatmentof unmodified Jackfruit seeds (UJS) with hydrochloric acid. Both UJS and MJS were characterized by FT-IR which showed increased in the number of negatively charged functional groups responsible for Cr^{3+} ions adsorption. Adsorption parameters (pH, contact time, adsorbent dose and initial concentration) greatly influenced the adsorption process. The Langmuir adsorption model was best fitted with experimental value with R^2>0.99, which assumed monolayer coverage of adsorbed Cr^{3+} ions with a maximum adsorption capacity of 16.18 mg g^{-1} (MJS) and 10.34 mg g^{-1} (UJS). The time data fitted well in pseudo-second order kinetic model with R^2>0.99 with rate constant (k_2) and calculated q_e higher in MJS compared to UJS. From the results of the study, JS adsorbent proved to be a cheap, alternative, effective and environmentally friendly adsorbent for Cr^{3+} ions adsorption from aqueous solution.**

Keywords: **Cr^{3+}, Adsorption,*Artocarpus heterophyllus* L. seeds, Isotherm, Kinetic**

I. INTRODUCTION

Presence of chromium and its chemical forms beyond permissible levels is toxic to the environment [1]. Cr^{3+}, an industrial waste from dyes and pigments manufacturing [2], wood preservation [3] and leather-tanning [4]enters to the water bodies making water unsafe for consumption to both aquatic organisms and human beings. Although, it is less toxic, when oxidized to Cr^{6+} in body tissues by oxidants, it becomes mutagenic and carcinogenic to living organisms [5,6] causing serious health effects in human beings such as lung cancer, liver and kidney damages, skin irritation and stomach injuries [8].According to United states Environmental Protection Agency (US EPA)drinking water standards, the maximum permissible limit of total chromium content in drinking water is 0.1 mg/L [7].Many physio-chemical technologiesincluding ion exchange [8,9]chemical precipitation [10]membrane filtration [11] and electrodialysis [12] have been conventionally used in the removal of Cr^{3+}ions from water. These methods have however remained expensive, low removal efficiency, ineffective in the removal of Cr^{3+} ions at trace concentrations ranging 1-100 mg/L[4]and production of chemical sludge [13]. Coming up with a novel, cost effective, easy in design and operation and environmentally friendly technique that suit the needs of communities is paramount. Adsorption has increased research interest and the most versatile technique because of its effectiveness, simplicity and economical in water purification [11]. The use of biomass from agricultural wastes such as Jackfruit seeds [14], Watermelon peels [15], orange and banana peels [16], banana peels [17] amongst others in heavy metals removalhas increased research interest because of their availability in large quantities [18].This provides an alternative method for water purification.

Application of these biowastes in their raw forms in drinking water treatment have been reported to have a low adsorption capacity in metal ions uptake [14]. They have also caused leaching of organic matter containing tannin compounds and other colouring agents which affecting taste and colour of the treated water and an increasedchemical oxygen demand (COD)[19,24].Chemical treatment has reported to solve the above challenge. Studies have been carried out on the use of modified biowastes in the removal of Cr^{3+} ions from wastewater. Dos Santos and co-workers treated sugarcane bagasse with sodium hydroxide and citric acid improved uptake of Cr^{3+} ions to maximum adsorption capacity of 58.00 mg g^{-1} from 20.34 mg g^{-1} in raw adsorbent [20]. In another study, removal of Cr^{3+} ions by activated charcoal increased from 7.51 mg g^{-1} to 9.99 mg g^{-1} as the temperature increased to 37.5 ^oC from 10 ^oC [21]. Atieh and co-researchers on adsorption of the metal ions using Nitric acid modified carbon nanotubes reported that the adsorption process fitted Freundlich isotherm model with an adsorption capacity of 0.5 mg g^{-1} for modified adsorbent compared to 0.3718 mg g^{-1} for acid treated adsorbent [22].

Chemical modification of biowastes using mineral acids have been reported to enhance the number of negatively charged adsorbent sites enhancing adsorption capacity [19]. The proposed mechanism of HCl acid modification of cellulose is as represented in the scheme below [26]:

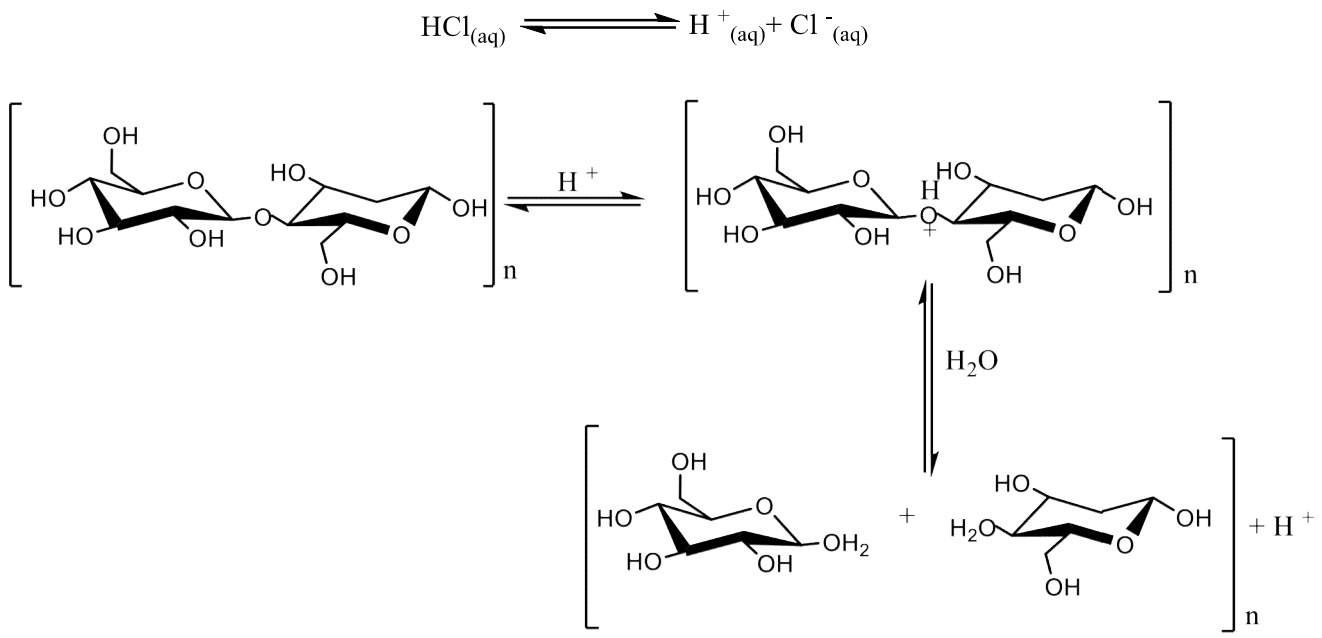

Huang and co-authors used nitric acid as a modifying agent for lignite and they noticed an increase in hydroxyl, carbonyl, and carboxyl polar oxygen containing functional groups which increased negatively charged functionality properties which enhanced metal ion adsorption performance [23].In a different study, activated carbon surface modification hydrochloric acid increased the number of oxygen complexes which improved the adsorption of Cr^{6+} ions [25]. The present work involved chemically modifying Jackfruit seeds with hydrochloric acid for the biosorption of Cr^{3+} ions from aqueous solution. The effect of pH, contact time, adsorbent dose and initial Cr^{3+}ions concentration was investigated. Isotherm and kinetic models were employed for the determination of adsorption capacity and kinetic parameters respectively.

II. MATERIALS AND METHODS

2.1 Materials

All the chemicals and reagents used were of analytical grade. Chromium Nitrate, Cr $(NO_3)_3$. $9H_2O$, Sodium Acetate ($C_2H_3O_2Na$), Hydrochloric acid (HCl) and Sodium hydroxide (NaOH) were commercially purchased from Sigma Aldrich (Kobian, Nairobi Kenya). Jackfruits *Artocarpus heterophyllus* L.were collected from City Park market, Nairobi, Kenya.

2.2 Adsorbate preparation

A 1000 mg L^{-1} stock solution of Cr^{3+} ions was prepared in $C_2H_3O_2Na$ buffer solution to maintain a constant ionic strength. Distilled water was used in all the subsequent experiments. Working solutions were obtained through dilution with distilled water. Fresh dilutions were prepared and used for each batch experiment. 1.0×10^{-1} mol $dm^{-3}$of HCl or NaOH solutions were used to adjust the pH of working Cr^{3+}solutions.

2.3 Adsorbent preparation

Jackfruits were cut open and seeds sample were washed with distilled water, oven dried at 105°C for 24 hours, were grounded and sieved through a fine-mesh sieve (150 to 250 mm) and kept in an air tied bottle labeled as unmodified Jackfruit seeds (UJS) awaiting subsequent experiments. Chemical modification was performed as described by [27] with slight adjustments. 5 g of UJS was shaken with 100 mL of 0.5 M HCl at 300 rpm for four hours. The mixture was then filtered in sintered glass crucible and *vacuo* dried at a room temperature. The dried adsorbent was stored in airtight bottle labelled as modified Jackfruit seeds (MJS).

2.4 Instrumentation

FT-IR (IRTracer-100, SHIMADZU made in Japan) model was used to determine the functional groups present in both UJS and MJS. Lab-line mechanical reciprocating shaker model SSL_2 (Harrogate, UK) was used for batch experiments. pH meter (HANNA model) was used to adjust pH of Cr^{3+} solution. AAS (AA-6200, SHIMADZU) model was used to determine the Cr^{3+} ions content in the supernatant solution.

2.5 FTIR Analysis

FTIR spectra was adjusted to % Transmission mode and were recorded at a mid-range of 4000-500 cm^{-1} at a room temperature with a resolution of 10 scans per every single spectrum.

2.6 Adsorption experiments

Batch adsorption experiments were performed at 25±1°C on a mechanical shaker at 150 rpm using 100 mL screw plastic bottles.Various influencing adsorption parameters such as pH, contact time, adsorbent dosage and initial Cr^{3+} ions concentrationwere varied.

2.6.1 Effect of pH

The influence of changing pH on Cr^{3+} ions uptake by UJS and MJS were studied by putting 0.02 ± 0.0005g of each of the adsorbent into 100 mL screw plastic bottles containing 10 mL of 20 mg L^{-1} of Cr^{3+} ions adjusted to pH range (2.0-7.0) by 1.0×10^{-1} mol dm^{-3} of HCl or NaOH. The mixture was agitated, filtered and the concentration of Cr^{3+}ionsin the supernatant metal solution was determined by AAS.

2.6.2 Effect of contact time

Effect of contact time on the adsorption of Cr^{3+} ions were studied through mixing 10 mL of 20 mg L^{-1} of Cr^{3+} ions at optimal pH with 0.02 ± 0.0005 g of each of UJS and MJS adsorbent. The respective mixtures were allowed to equilibrate after agitating at different time intervals (0-150 minutes). The solid material was filtered off through suction and the concentration of Cr^{3+} ions in the filtrate determined.

2.6.3 Effect of adsorbent dose

The effect of UJS and MJS dose on Cr^{3+} ions uptake on 10 mL of 20 mg L^{-1} metal solution was demonstrated by batch technique of varied dosages (0.01–0.03 ± 0.0005 g). Optimum conditions of pH = 5 and contact time = 60 minutes (UJS); 40 minutes (MJS) were used. The mixtures were equilibrated, filtered and amount of residual Cr^{3+} ions analysed.

2.6.4 Effect of Cr^{3+} ions concentration

The initial Cr^{3+} ions concentration effect was carried out using 10 mL of various optimal metal ion concentrations (5-200 mg L^{-1}) mixed with optimal dose of 0.02 ± 0.0005 g of each of UJS and MJS. The mixtures were then agitated for 60 minutes (UJS); 40 minutes (MJS). Filtration was done and Cr^{3+} ions concentration in the supernatant solution was determined.

2.7 Data evaluation

The amount of Cr^{3+} ions adsorbed at equilibrium was calculated by equation 1:

$$q_e = \frac{C_i - C_e}{M} V \quad (1)$$

Where $q_e$is the amount of metal ions adsorbed at equilibrium, C_i is initial adsorbate concentration and $C_e$is adsorbate final concentration at equilibrium (mg/L), V is the total volume of the solution and M is the adsorbent dosage mass[14].

2.8 Adsorption isotherm models

To determine adsorption capacity of UJS and MJS on adsorption of Cr^{3+} ions, concentration equilibrium data was fitted into Langmuir and Freundlich isotherm models. Langmuir isotherm models describes a monolayer interaction which is chemisorption in nature [39]. Its linearized is given by the equation 2:

$$\frac{C_e}{q_e} = \frac{C_e}{Q_m} + \frac{1}{Q_m b} \quad (2)$$

Where $C_e$is the concentration of Cr^{3+} ions at equilibrium (mg L^{-1}), Q_e is the amount of Cr^{3+} ions adsorbed per unit weight of the adsorbent (mg g^{-1}) at equilibrium, constants Q_m and b are the adsorption capacity (mg g^{-1}) and b is the energy of the adsorption (L mg^{-1}) respectively. A plot of $\frac{C_e}{q_e}$against $C_e$gives a linear plot used to obtain Q_m and b. Freundlich isotherm model describes a multilayer adsorption and an exclusively physisorption process. Its linearized equation is given by the equation 3:

$$\ln q_e = \ln K_F + \frac{1}{n} ln\, C_e \quad (3)$$

Where$q_e$is the amount of Cr^{3+} ions adsorbed (mg/L) at equilibrium, $C_e$is the concentration of Cr^{3+} ions at equilibrium (mg/L). K_F and n is adsorption capacity and adsorption intensity constant respectively. A plot of lnq_e against lnc_e gives a straight line and is used to determine K_F and n from the intercept and slope.

2.9 Adsorption Kinetic models

To determine adsorption rate and mechanisms, the kinetic time data was fitted into pseudo-first-order and pseudo-second-order kinetic models. Linearized kinetic rate equation for pseudo-first-order model can be written a given by equation 4:

$$\ln(q_e - q_t) = \ln q_e - k_1\, t \quad (4)$$

Wherek_1 is the rate constant, q_e is the adsorption capacity at equilibrium and $q_t$is the adsorption capacity at time (t). A linear plot of ln (q_e-q_t) against time (t) results in a straight line with -$k_1$as the slope and the ln $q_e$as the intercept and can be used to obtain $k_1$and q_e calculated value. Linearized kinetic rate equation for pseudo-second-order model can be written a given by equation 5:

$$\frac{t}{q_t} = \frac{1}{k_2\, q_e^2} + \frac{t}{q_e} \quad (5)$$

where $k_2$is the rate constant. Linear plot of t/q_tagainst time (t) yields a linear line with $1/q_e$ as the slope and $1/k_2 q_e{}^2$as the intercept used to calculate q_e(calculated) value and k_2.

III. RESULTS AND DISCUSSIONS

3.1 FTIR Analysis

FTIR spectrum of unmodified and modified Jackfruit seeds adsorbent is presented by figure 1:

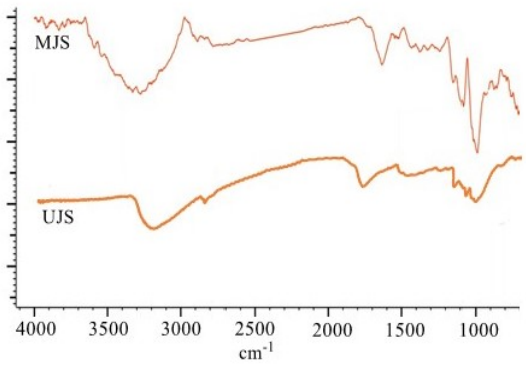

Fig-1: FTIR spectrum of unmodified Jackfruit seeds (UJS) and modified Jackfruit seeds (MJS)

Chemical treatment of UJS indicated only shifting and increased intensity of the functional groups. The band occurring at 3345 cm^{-1} (UJS) and 3287 cm^{-1} (MJS) is ascribed to hydroxyl groups (-OH) stretching vibrations of alcoholic and carboxylic acid groups [40]. MJS showed an increased broadness of the peak indicating increased carboxylic and alcoholic –OH groups [27]. A weak peak at 2910 cm^{-1} (UJS) and 2924 cm^{-1} (MJS) is attributed to symmetric and asymmetric sp^3 –CH stretching vibrations [41]. The difference in adsorption bands at 1785 cm^{-1} and 1762 cm^{-1} associated with carbonyl groups (-C=O) in UJS and MJS is due to structural changes that occur as a result of acid treatment [15]. Peaks at 1200 – 1000 cm^{-1} could be attributed by C-O stretching vibrations of carboxylic acid and alcoholic groups respectively [14]. Hydroxyl (-OH) groups, carbonyl (-C=O) groups and carboxylic ($-COO^-$) groups in UJS are important adsorption sites for Cr^{3+} ions removal. The intensities of the peaks after acid treatment is increased due to an increase in negatively charged adsorbent sites. Therefore, the adsorption capacity is expected to be high in MJS than UJS.

Optimization

Effect of pH

The effect of pH on the adsorption of Cr^{3+} was investigated by varying pH (2-7) and results presented by figure 2 below:

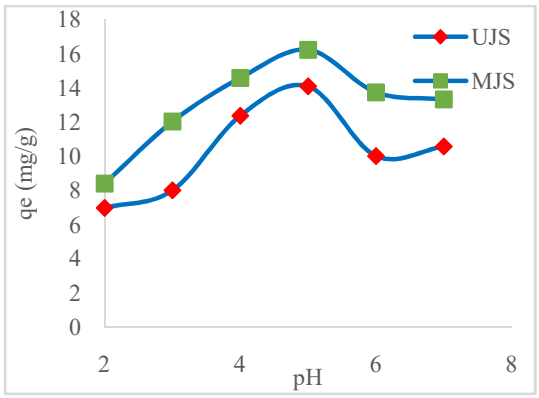

Fig-2: Effect of pH on adsorption of Cr^{3+} ions on UJS and MJS

pH is crucial in determining the adsorbent surface charge and the chemistry of the metal ions in the solution [14]. The results in figure 2 show an increased adsorption capacity of Cr^{3+} ions with increase in pH to optimal value of 5. Low adsorption capacity at lower pH's may be due to protonation of UJS and MJS surfaces due to increased H_3O^+ ions in the metal solution. This makes the adsorbent less available for Cr^{3+} ions adsorption [28]. Low Adsorption capacity at pH>5 may be due to precipitation of Cr^{3+} ions by excess of hydroxyl groups in the metal solution. This reduces the number of Cr^{3+} ions in the solution to be complexed by the adsorption sites [22]. This is in agreement with Cr^{3+} speciation with pH diagram [3, 20,29].

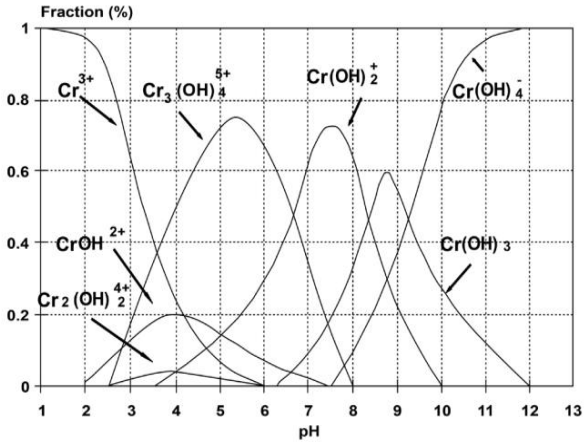

At pH<3.6, Cr^{3+}ions exist, at pH>4 and <6.5, $Cr(OH)^{2+}$and $Cr(OH)^{2+}$ions exist. However, atpH between 7-12, neutral Cr $(OH)_3$ species exist andthis lowers the amount of Cr^{3+} in metal solution as well as adsorption affinity decreasing the adsorption capacity [31]. The results agree with those reported by [29].

Effect of contact time

Studies of contact time were conducted by varying time at intervals of 20 minutes and results are presented by the figure 3 below:

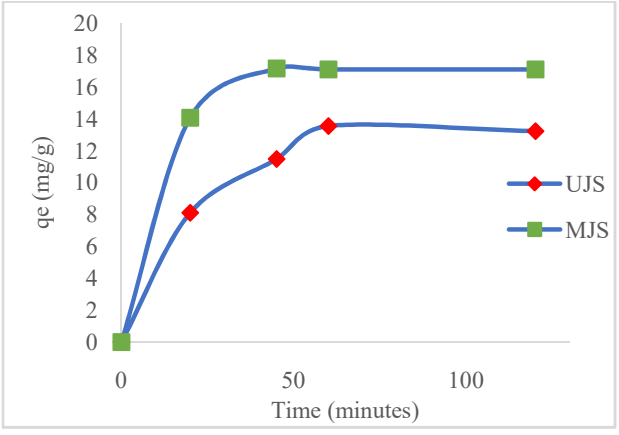

Fig-3: Effect of contact time on adsorption of Cr^{3+} ions on UJS and MJS

Figure 3 shows Cr^{3+} ions adsorption on the UJS and MJS as a function of contact time. The results showed a rapid adsorption of Cr^{3+} ions within the first 60 minutes for the raw Jackfruit seeds adsorbents and 40 minutes for the modified Jackfruit seeds adsorbent beyond which a steady state is observed. Rapid adsorption was expected as more number of binding sites are initially available for adsorption of Cr^{3+} ions which are eventually used up leading to a steady state [32]. Results show greater removal capacity by acid modified adsorbent than raw adsorbent. This can be attributed to enhanced surface polarity after acid modification. The study compare with those reported by [22, 35, 37].

Effect of adsorbent dose

The adsorption capacity for Cr^{3+} ions as a function of adsorbent dose is shown by the figure 4:

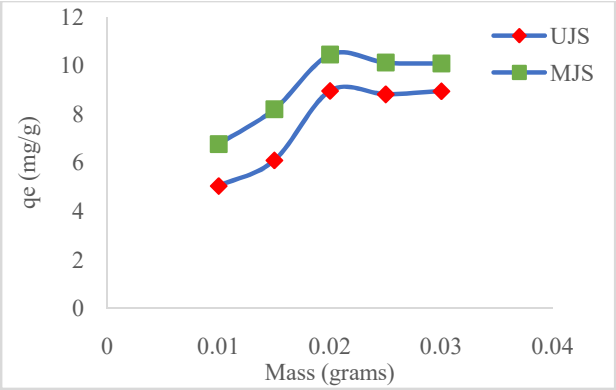

Fig-4: Effect of adsorbent dose on adsorption of Cr^{3+} ions on UJS and MJS

The results in the figure 4 above showed an increased adsorption capacity (0.01-0.02 g) beyond this optimum dose limit (0.02 g) no significant increase is observed. Increasing adsorbent dose increases the adsorbing groups available on the adsorbent surface and this provides adsorption sites for Cr^{3+} ions uptake increasing adsorption capacity [33]. A plateau beyond optimal dose may be attributed to overlapping or aggregation of adsorption sites that results in the increase of diffusion path length and decreases the total adsorbent surface area which is available to the metal ions[34]. The study compare with those reported by [36].

Effect of initial concentration

The influence of initial concentration on Cr^{3+} ions via unmodified and modified Jackfruit seeds was probed by varying the concentration from 5-200 mg L^{-1} while keeping other parameters constant. The results are presented by the figure 5:

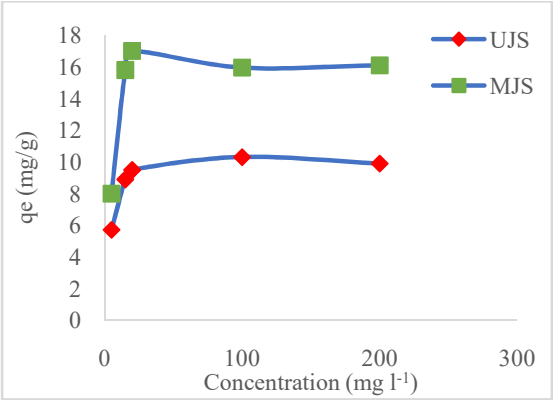

Fig-5: Effect of initial concentration on adsorption of Cr^{3+} ions on UJS and MJS

It was observed that adsorption capacity increased with increase in concentration to an optimal concentration of 20 mg L^{-1} beyond which a steady state was observed. The phenomenon is explained by the fact that at low concentrations, all metal ions are almost adsorbed by the available active sites but further increased concentration leads to saturation of the binding sites making more Cr^{3+} ions left in the solution [14, 15]. The results agree with those reported by [38].

Adsorption capacity

The adsorption capacity of Cr^{3+} ions onto UJS and MJS was analyzed using Langmuir and Freundlich isotherm models and results are tabulated by the table 1:

Table 1: Langmuir and Freundlich constants for Cr^{3+} ions adsorption using UJS and MJS adsorbents

Ads	Langmuir Isotherm			Freundlich Isotherm			
	Q_m (mg/g)	b (l/g)	R^2	K_F (mg/g)	n	R^2	Best model
UJS	10.34	0.4115	0.9985	5.74	7.8989	0.8599	**Langmuir**
MJS	16.18	0.2876	0.9996	6.91	4.9975	0.9170	**Langmuir**

Langmuir isotherm plots showed a better correlation with the experimental data than Freundlich isotherm plots as shown by the figure (6). Correlation coefficient (R^2) values were >0.99 for Langmuir and this showed that adsorption of Cr^{3+} ions on UJS and MJS adsorbents was well explained by Langmuir isotherm which assumes a monolayer adsorption and a chemisorption process [35]. The values of b of 0.4115 and 0.2876 for UJS and MJS indicated favorability of the adsorption process. Adsorption capacities of UJS were low than those of MJS. This was due to the effect of acid modification. These results compare with those reported by [14, 28, 34, 42].

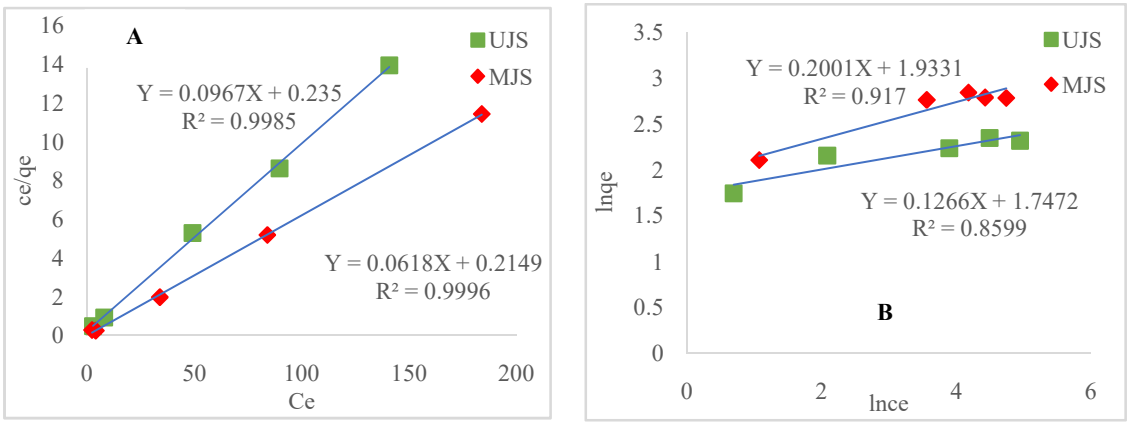

Fig-6: Langmuir (A) and Freundlich (B) Isotherm plots for UJS and MJS

A comparable adsorption capacity of the UJS and MJS adsorbents with other low-cost adsorbents for Cr^{3+} ions removals is shown in table 2:

Table 2. Adsorption capacity of different adsorbent materials for the adsorption of Cr^{3+} ions

Adsorbent	Q_m (mg/g)	b (l/g)	R^2	Reference
Rubber tire (Activated carbon)	12.08	0.17	0.9900	[35]
Olive wastes (Activated carbon)	12.46	0.08	0.9900	[43]
Water hyacinth	6.61	0.05	0.9570	[44]
Modified rice husk	4.74	0.01	0.9900	[45]
Sorghum straw	9.35	0.12	0.9600	[46]
Corn stalk	7.30	0.64	0.9931	[47]
Chinese reed	1.85	0.20	0.9841	[48]
Sphagnum moss peat	7.55	0.30	0.9980	[49]
Rhodococcus opacus bacteria	1.40	1.08	0.9292	[50]
UJS	10.34	0.41	0.9985	This study
MJS	16.18	0.29	0.9996	This study

Adsorption kinetics

The adsorption kinetics of Cr^{3+} ions onto UJS and MJS was analyzed using pseudo-first-order and pseudo-second-order and results are presented by the table 3:

Table 3:Pseudo-first-order and Pseudo-second-order constants for Cr^{3+} ions adsorption using UJS and MJS adsorbents

Ads	Pseudo-first-order				Pseudo-second-order			
	q_e, exp (mg g^{-1})	q_e, cal (mg g^{-1})	K_1 (mgg^{-1} min^{-1})	R^2	q_e, cal (mg g^{-1})	K_2 (mgg^{-1} min^{-1})	R^2	Best model
UJS	14.63	8.19	2.68×10^{-2}	0.7930	14.45	4.92×10^{-2}	0.9975	**Pseudo-second-order**
MJS	17.36	3.21	2.06×10^{-2}	0.5978	17.27	6.77×10^{-2}	0.9993	**Pseudo-second-order**

Pseudo-second-order kinetic plots showed better linearity of experimental time data compared to pseudo-first-order plots (figure 7). Kinetic data shows R^2 values are 0.7930 and 0.5978 for pseudo-first-order model and 0.9975 and 0.9993 for pseudo-second-order model for UJS and MJS respectively. Pseudo-second-order R^2 values are in agreement with R^2>0.99 for both UJS and MJS. Also, experimental q_e values are closer to calculated q_e values as compared to those in pseudo-first-order. These results revealed that pseudo-second-order best fitted in explaining the adsorption of Cr^{3+} ions using UJS and MJS. The modelassumes chemisorption as the rate determining step that controlled the adsorption process [15,42]. MJS recorded higher values of calculated q_e and k_2 compared to UJS. The results compare with those reported by [20,42,49,50].

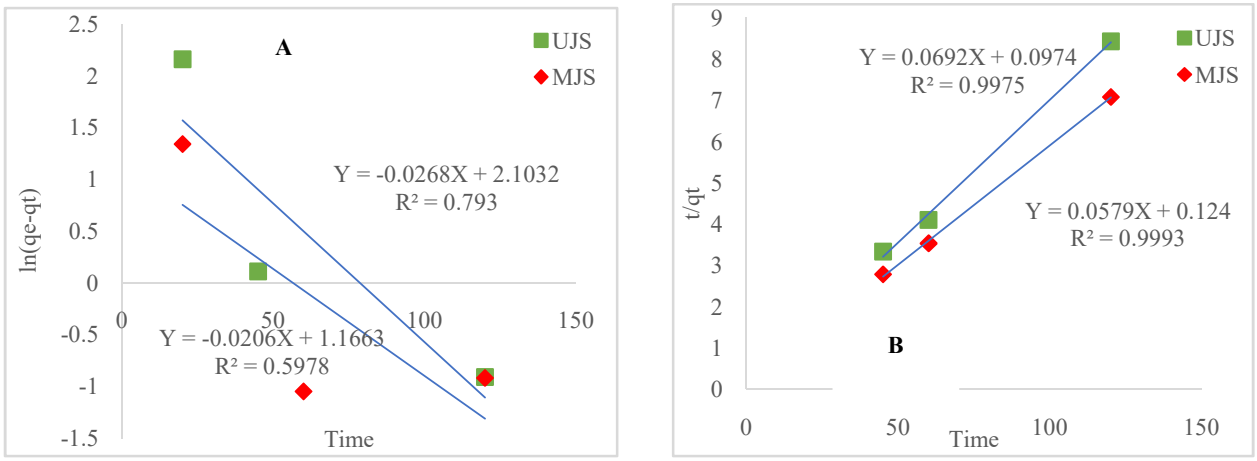

Fig-7: Pseudo-first-order (A) and Pseudo-second-order (B) kinetic plots for UJS and MJS

IV. CONCLUSION

In the present work, unmodified Jackfruit seeds adsorbent (UJS) was chemically treated with hydrochloric acid. FT-IR analysis showed more intense peaks which indicated an increase in the number of functional groups in modified Jackfruit seeds (MJS) for Cr^{3+} ions adsorption. The adsorption process was greatly influenced by adsorption parameters of pH, contact time, adsorbent dose and initial concentration. The equilibrium and kinetic studies of adsorption Cr^{3+} ions onto UJS and MJS was studied. The concentration data were analyzed by Langmuir and Freundlich isotherm models and it was found that adsorption of Cr^{3+} ions was well described by Langmuir isotherm model which implied chemical interaction between Cr^{3+} ions and adsorbent sites. Time data was analyzed by pseudo-first-order and pseudo-second-order kinetic models. Pseudo-second-order fitted well in describing adsorption of Cr^{3+} ions and that chemisorption was the rate-determining step.

ACKNOWLEDGEMENTS

The authors express their gratitude to Dedan Kimathi University of Technology for chemicals, reagents and solvents, laboratory space and equipment. Also to Kenyatta University for FT-IR and AAS analysis.

REFERENCES

[1]. **Mekonnen, E., Yitbarek, M. and Soreta, T.R. (2015).** Kinetic and Thermodynamic Studies of the Adsorption of Cr (VI) onto Some Selected Local Adsorbents. *South African Journal of Chemistry*, **68**: 45–52.

[2]. **Gupta, V. K., Agarwal, S. and Saleh, T. A. (2011).** Chromium removal by combining the magnetic properties of iron oxide with adsorption properties of carbon nanotubes. *Water Research*, **45** (6): 2207–2212.

[3]. **Wang, J., Zhang, D., Liu, S. and Wang, C. (2020).** Enhanced removal of chromium (III) for aqueous solution by EDTA modified attapulgite: Adsorption performance and mechanism. *Science of the total environment*, **720**: 1-8.

[4]. **Blázquez, G., Calero, M., Hernáinz, F., Tenorio, G. & Martín-Lara, M. A. (2010).** Batch and continuous packed column studies of chromium (III) biosorption by olive stone. *Environmental Progress & Sustainable Energy*, **30** (4): 576–585.

[5]. **Jiang, X., Fan, W., Li, C., Wang, Y., Bai, J., Yang, H. & Liu, X. (2019).** Removal of Cr (VI) from wastewater by a two-step method of oxalic acid reduction-modified fly ash adsorption. *RSC Advances*, **9** (58): 33949–33956.

[6]. **Anupam, K., Dutta, S., Bhattacharjee, C. and Datta, S. (2011).** Adsorptive removal of chromium (VI) from aqueous solution over powdered activated carbon: Optimisation through response surface methodology. *Chemical Engineering Journal*, **173** (1): 135–143.

[7]. **US EPA, (2011).** Ground Water and Drinking Water, Current Drinking Water Standards, EPA 816-F-02

[8]. **Bagheri, M., Younesi, H., Hajati, S. & Borghei, S. M. (2015).** Application of chitosan-citric acid nanoparticles for removal of chromium (VI). *International Journal of Biological Macromolecules*, **80**: 431–444.

[9]. **Marzouk, I., Hannachi, C., Dammak, L. & Hamrouni, B. (2011).** Removal of chromium by adsorption on activated alumina. *Desalination and Water Treatment*, **26** (1-3): 279–286.

[10]. **Shariati, S., Khabazipour, M. & Safa, F. (2016).** Synthesis and application of amine functionalized silica mesoporous magnetite nanoparticles for removal of chromium (VI) from aqueous solutions. *Journal of Porous Materials*, **24** (1): 129–139.

[11]. **Kumari, M., Pittman, C. U. and Mohan, D. (2015).** Heavy metals [chromium (VI) and lead (II)] removal from water using mesoporous magnetite (Fe3O4) nanospheres. *Journal of Colloid and Interface Science*, **442**: 120–132.

[12]. **Ballav, N., Maity, A. & Mishra, S. B. (2012).** High efficient removal of chromium (VI) using glycine doped polypyrrole adsorbent from aqueous solution. *Chemical Engineering Journal*, **198-199**: 536–546.

[13]. **Shen, C., Chen, H., Wu, S., Wen, Y., Li, L., Jiang, Z., Li, M. & Liu, W. (2013).** Highly efficient detoxification of Cr (VI) by chitosan–Fe (III) complex: Process and mechanism studies. *Journal of Hazardous Materials*, **244-245:** 689–697.

[14]. **Ndung'u S. N., Wanjau R.N., Nthiga E.W., Ndiritu J. and Mbugua G.W. (2020).** Complexation equilibrium studies of Cu^{2+}, Cd^{2+} and Pb^{2+} ions onto ethylenediamine quaternised *Artocarpus heterophyllus* L. seeds from aqueous solution. *IOSR Journal of applied chemistry (IOSR-JAC)*, **13** (12): 01-12.

[15]. **Wanja, N.E., Murungi, J., Ali, A.H. and Wanjau, R. (2016).** Efficacy of Adsorption of Cu (II), Pb (II) and Cd (II) Ions onto Acid Activated Watermelon Peels Biomass from Water. *International Journal of Science and Research*, **5** (8): 671- 679.

[16]. **Pakshirajan, K., Worku, A. N., Acheampong, M. A., Lubberding, H. J. & Lens, P. N. L. (2013).** Cr (III) and Cr (VI) removal from aqueous solutions by cheaply available fruit waste and algal biomass. *Applied biochemistry and biotechnology*, **170** (3): 498–513.

[17]. **Ali, A., Saeed, K. & Mabood, F. (2016).** Removal of chromium (VI) from aqueous medium using chemically modified banana

peels as efficient low-cost adsorbent. *Alexandria Engineering Journal*, **55** (3): 2933–2942.

[18]. **Thakuria, M.N. and Talukdar, A.K. (2012).** Removal of Chromium (III) from drinking water using ash of bark of *Terminalia arjuna*. *Asian Journal of Research in Chemistry*, **5** (4): 541-546.

[19]. **Pandey, R., Ansari, N. G., Prasad, R. L. & Murthy, R. C. (2014).** Removal of Cd (II) ions from simulated wastewater by HCl modified *Cucumis sativus* peel: Equilibrium and Kinetic study. *Air, Soil and Water Research*, **7**: 93-101.

[20]. **Dos Santos, V., Dragunski, A., Tarley, D. & Caetano, J. (2012).** Highly improved Chromium (III) uptake capacity in modified sugarcane bagasse using different chemical treatments. *Química Nova*, **35** (8): 1606-1611.

[21]. Abdulla, F.H. (2014). Removal of Chromium (III) ions from its aqueous solution on adsorbent surfaces: Charcoal, Attapulgite and Date Palm leaflet powder. *Iraqi Journal of Science*, **55** (4): 1415-1430.

[22]. **Atieh, M. A., Bakather, O. Y., Tawabini, B. S., Bukhari, A. A., Khaled, M., Alharthi, M., Fettouhi, M. & Abuilaiwi, F. A. (2010).** Removal of Chromium (III) from water by using modified and nonmodified carbon nanotubes. *Journal of Nanomaterials*, **2010**: 1–9.

[23]. **Huang, B., Liu, G., Wang, P., Zhao, X. & Xu, H. (2019).** Effect of nitric acid modification on characteristics and adsorption properties of lignite. *Processes*, **7** (3): 167-182.

[24]. **Abdolali, A., Guo, W. S., Ngo, H. H., Chen, S. S., Nguyen, N. C. and Tung, K. L. (2014).** Typical lignocellulosic wastes and by-products for biosorption process in water and wastewater treatment: A critical review. *Bioresource Technology*, **160**: 57–66.

[25]. **Park, S.J. & Jang, Y.S., (2002).** Pore structure and surface properties of chemically modified activated carbons for adsorption mechanism and rate of Cr (VI). J. Colloid Interface Science, **249** (2): 458–463.

[26]. **Braun, B. & Dorgan, J.R. (2009).** Single-step method for the isolation and surface functionalization of cellulosic nanowhiskers. *Biomacromolecules*, **10**:334–341

[27]. **Assirey, E.A., Sirry, S.M., Burkani, H.A. & Ibrahim, M.A. (2020).** Modified *Ziziphus spina-christi* stones as green route for the removal of heavy metals. *Scientific reports*, **10** (1): 1-10.

[28]. **Pimentel, P. M., Oliveira, R. M. P. B., Melo, D. M. A., Melo, M. A. F., Assunção, A. L. C. & Gonzales, G. (2011).** Adsorption of chromium ions on oil shale waste. *Brazilian journal of petroleum and gas*, **5** (2): 65-73.

[29]. **Lu, Z., Wang, H., Li, J., Yuan, L. & Zhu, L. (2015).** Adsorption characteristics of bio-adsorbent on chromium (III) in industrial wastewater. *Water Science and Technology*, **72** (7): 1051–1061.

[30]. **Zhang, N., Suleiman, J. S., He, M. & Hu, B. (2008).** Chromium (III)-imprinted silica gel for speciation analysis of chromium in environmental water samples with ICP-MS detection. *Talanta*, **75** (2): 536–543.

[31]. **Saleh, T.A. & Gupta, V.K. (2011).** Synthesis of MWCNT/MnO2 and their application for simultaneous oxidation of arsenite and sorption of arsenate. *Applied Catalysis B: Environmental*, **106** (1–2): 46–53.

[32]. **Krishna Mohan, G. V., Naga Babu, A., Kalpana, K. & Ravindhranath, K. (2017).** Removal of chromium (VI) from water using adsorbent derived from spent coffee grounds. *International Journal of Environmental Science and Technology*, doi:10.1007/s13762-017-1593-7

[33]. **Moftakhar, M. K., Yaftian, M. R. and Ghorbanloo, M. (2016).** Adsorption efficiency, thermodynamics and kinetics of Schiff base-modified nanoparticles for removal of heavy metals. *International Journal of Environmental Science and Technology*, **13** (7): 1707–1722.

[34]. **Maleki, A., Pajootan, E. & Hayati, B. (2015).** Ethyl acrylate grafted chitosan for heavy metal removal from wastewater: Equilibrium, kinetic and thermodynamic studies. *Journal of the Taiwan Institute of Chemical Engineers*, **51**: 127–134.

[35]. **Gupta, V. K., Ali, I., Saleh, T. A., Siddiqui, M. N. & Agarwal, S. (2012).** Chromium removal from water by activated carbon developed from waste rubber tires. *Environmental Science and Pollution Research*, **20** (3): 1261–1268.

[36]. **Masoumi, A. & Ghaemy, M. (2014).** Removal of metal ions from water using nanohydrogel tragacanth gum-g-polyamidoxime: Isotherm and kinetic study. *Carbohydrate Polymers*, **108**: 206–215.

[37]. **Bayazit, T.S. & Kerkez, Ö. (2014).** Hexavalent chromium adsorption on superparamagnetic multi-wall carbon nanotubes and activated carbon composites. *Chemical Engineering Research and Design*, **92** (11): 2725–2733.

[38]. **Gu, M., Hao, L., Wang, Y., Li, X., Chen, Y., Li, W. & Jiang, L. (2020).** The selective heavy metal ions adsorption of zinc oxide nanoparticles from dental wastewater. *Chemical Physics*, **534**: 1-8.

[39]. **Zhu, H.-X., Cao, X.-J., He, Y.-C., Kong, Q.-P., He, H. & Wang, J. (2015).** Removal of Cu^{2+} from aqueous solutions by the novel modified bagasse pulp cellulose: Kinetics, isotherm and mechanism. *Carbohydrate Polymers*, **129**: 115–126.

[40]. **Jahromi, F.G. & Ghahreman, A. (2019).** Effect of Surface Modification with Different Acids on the Functional Groups of AF 5 Catalyst and Its Catalytic Effect on the Atmospheric Leaching of Enargite. *Colloids and Interfaces*, **3** (2): 45-60.

[41]. **Ndiritu J., Mwangi I.W., Murungi J. I., Wanjau R. N. (2020).** Uptake of p-Nitrophenol (PNP) from model aqueous solutions using raw and quaternised *Afromomum melegueta* peels. *African Journal of Pure Applied Sciences*, **1** (1): 01 – 08.

[42]. **Pietrelli, L., Francolini, I., Piozzi, A., Sighicelli, M., Silvestro, I. & Vocciante, M. (2020).** Chromium (III) Removal from Wastewater by Chitosan Flakes. *Applied Sciences*, **10** (6): 1925-1935.

[43]. **Seydoun, B., Karima, E., Abdelrani, Y., Abdelhakim, A. & Abdelaziz, B. (2018).** Activated Carbon from Olive Wastes as an Adsorbent for Chromium ions removal.*Iranian Journal of Chemistry and Chemical Engineering*, **37** (6):107-123.

[44]. **Elangovan, R., Philip, L. & Chandraraj, K. (2008).** Biosorption of chromium species by aquatic weeds: Kinetics and mechanism studies. *Journal of Hazardous Materials*, **152** (1): 100–112.

[45]. **Kanwal, F., Rehman, R., Mahmud, T., Anwar, J. & Ilyas, R. (2012).** Isothermal and thermodynamical modeling of Chromium (III) adsorption by composites of polyaniline with rice husk and saw dust. *Journal of the Chilean Chemical Society*, **57** (1): 1058-1063.

[46]. **Garcia-Reyes, R. B., & Rangel-Mendez, J. R. (2010).** Adsorption kinetics of chromium (III) ions on agro-waste materials. *Bioresource Technology*, **101** (21): 8099–8108.

[47]. **Bellú, S., García, S., González, J. C., Atria, A. M., Sala, L. F. & Signorella, S. (2008).** Removal of Chromium (VI) and Chromium (III) from Aqueous Solution by Grainless Stalk of Corn. *Separation Science and Technology*, **43** (11-12): 3200–3220.

[48]. **Namasivayam, C. & HÖll, W. H. (2004).** Chromium (III) removal in tannery waste waters using Chinese Reed (*Miscanthus Sinensis*), a fast growing plant. *European Journal of Wood and Wood Products*, **62** (1): 74–80.

[49]. **Balan, C., Bilba, D. & Macoveanu, M. (2009).** Studies on chromium (III) removal from aqueous solutions by sorption on Sphagnum moss peat. *Journal of the Serbian Chemical Society*, **74** (8-9): 953–964.

[50]. **Bueno, B. Y. M., Torem, M. L., Molina, F. & de Mesquita, L. M. S. (2008).** Biosorption of lead (II), chromium (III) and copper (II) by *R. opacus*: Equilibrium and kinetic studies. *Minerals Engineering*, **21** (1): 65–75.